PHYSICAL REVIEW B VOLUME 38, NUMBER 12 15 OCTOBER 1988-II

Dopant effect on intrinsic diffusivity in nickel silicide

H. Takai* and K. N. Tu
IBM Research Division, Thomas J. Watson Research Center, Yorktown Heights, New York 10598
(Received 25 April 1988)

The effect of P on the diffusivity of Ni and Si in Ni_2Si has been studied by analyzing the growth kinetics of Ni_2Si on P-doped and undoped polycrystalline Si films using W markers. The growth of Ni_2Si during the reaction of Ni and the P-doped Si films is faster than that of Ni and the undoped Si films. Marker analysis showed that the dopant does not affect the activation energies of diffusion; rather it increases greatly the preexponential factor of the diffusion of Si. The dopant effect has been examined in terms of the correlation factor and the entropy factor.

I. INTRODUCTION

Owing to widespread application of silicides together with doped polycrystalline silicon films as contacts and gates in the very-large-scale integrated Si technology, the interaction of dopant and silicide is of concern.[1,2] Since the dopant is an impurity to the silicide, the underlying issue of the interaction is related to the impurity effect on intrinsic diffusivities in an intermetallic compound. We report here a comparative study between the formation of Ni_2Si on undoped and phosphorus-doped polycrystalline Si with the objective of investigating the dopant effect, which has been quantitatively determined by employing marker analysis. We found that phosphorus enhanced the diffusion of Si in Ni_2Si by increasing the preexponential factor and at the same time slightly slowed down the diffusion of Ni, although Ni is the dominant diffusing species.

II. EXPERIMENT

The undoped and phosphorus-doped (8×10^{20} atoms/cm^3) polycrystalline Si films were prepared by the low-pressure chemical-vapor-deposition (LPCVD) technique on a 1300-Å-thick SiO_2 layer which was thermally grown on (100)-oriented Si wafers. The thickness of the polycrystalline films was 4000 Å. A sandwiched Ni/W/Ni film was deposited onto the polycrystalline Si substrates by electron-beam evaporation. The W film of nominal thickness of 3 Å, which serves as a diffusion marker, was deposited on a thin underlying Ni film of 200 Å in order to avoid the drag of the marker by the silicide/Si interface during silicide formation. These thin films were deposited consecutively without breaking the vacuum in a chamber. The top layer of Ni was 1300 Å thick (except for the phosphorus-doped polycrystalline Si substrate, on which 950 Å on Ni was deposited). The control of the W deposition is crucial to the experiment. If *W* is thick and continuous, it will be a barrier to the reaction between Ni and Si, and if W is too thin, it will be impossible to identify the marker position in the backscattering spectra. Another two sets of Ni films, 1400 Å thick without the W marker, were also deposited on the undoped and P-doped polycrystalline substrates as control samples for comparison.

We note that in this experiment four sets of samples have been prepared. By comparing the sets with and without the W marker, we can determine the influence of the marker on silicide formation. By comparing the sets with and without the P dopant, we can determine, through marker analysis, the effect of the dopant on intrinsic diffusivities in the silicide.

We also note that we have chosen to embed the W marker within the Ni film in the as-deposited state, in contrast to the earlier study of Ni_2Si formation, where an Xe marker was embedded within the Si substrate by ion implantation.[3] Since these markers are not located at the initial Ni/Si interface, they are not displaced until the silicide reaction front reaches them. The W marker will encounter the Ni_2Si/Ni interface while the Xe marker will encounter the Si/Ni_2Si interface before they are embedded into the silicide. Assuming no interfacial drag, once the marker is inside the silicide the direction and amount of marker displacement should be the same for the W and the Xe. On the other hand, if interfacial drag occurs, the direction of marker displacement of the W and the Xe will be opposite. Therefore, by comparing these two marker experiments, a definitive marker analysis can be obtained.

After deposition, the samples were isothermally annealed at temperatures between 200 and 300 °C for a period between 5 min and 4 h for Ni_2Si formation. The annealing was performed in a flowing-He tube furnace where the He was first passed through a bed of Ti held at 900 °C to remove residual oxygen in the gas. The partial pressure of oxygen in the tube furnace was estimated in the ($10^{-8}-10^{-9}$) Torr range.

Composition profiles and layer thicknesses of silicides and the W-marker displacement during silicide formation were measured by Rutherford backscattering with 2.3-MeV $^4He^+$ and by comparing the spectra to theoretical profiles generated by computer-simulation programs. The distribution profiles of phosphorus in the silicides and polycrystalline Si substrates were determined by secondary-ion mass spectroscopy (SIMS).

III. RESULTS

A. Growth kinetics of Ni_2Si without the W marker

Figures 1(a) and 1(b) show, respectively, Rutherford backscattering spectra (RBS) of Ni_2Si on the undoped

 ©1988 The American Physical Society

and phosphorus-doped polycrystalline Si substrates as a function of heat treatment time at 250 °C. These spectra indicate a layered compound growth. According to the plateau heights of the reacted layers, the composition of the reacted layers corresponds to that of Ni_2Si. These results and those obtained at other temperatures (not shown) indicate that the compound formed on both undoped and phosphorus-doped polycrystalline Si substrates are the same.

The thicknesses of silicide layer, x, measured from the width of the plateau on both substrates are plotted as a function of the square root of heat-treatment time, t, in Figs. 2(a) and 2(b), respectively. A straight line can be fitted to the data of each temperature and it passes through the origin, indicating that the Ni_2Si growth obeys a parabolic law and follows a diffusion-limited kinetic process. We chose to plot x versus $t^{1/2}$ instead of x^2 versus t because the measurement of t is much more accurate than x. The measurement of the latter is indirect and has a large uncertainty especially in the initial stage of reaction. Using the data presented in Fig. 2, the chemical interdiffusion coefficient $\tilde{D}$ is calculated from the relation of $x = 2\tilde{D}^{1/2}t^{1/2}$. Figure 3 shows an Arrhenius plot for Ni_2Si growth on the undoped and phosphorus-doped polycrystalline Si substrates. Straight lines can be fitted to the data for both substrates. From the relation of $\tilde{D}(T) = D_0\exp(-E_a/kT)$, where k is Boltzmann's constant and T is the absolute temperature; the activation energies E_a are found to be 1.23 and 1.22 eV for the undoped and the phosphorus-doped substrate, respectively, and the preexponential factors D_0 are found to be 5.37×10^{-2} and 5.05×10^{-2} cm^2/sec, respectively. The growth on the phosphorus-doped substrate is faster,

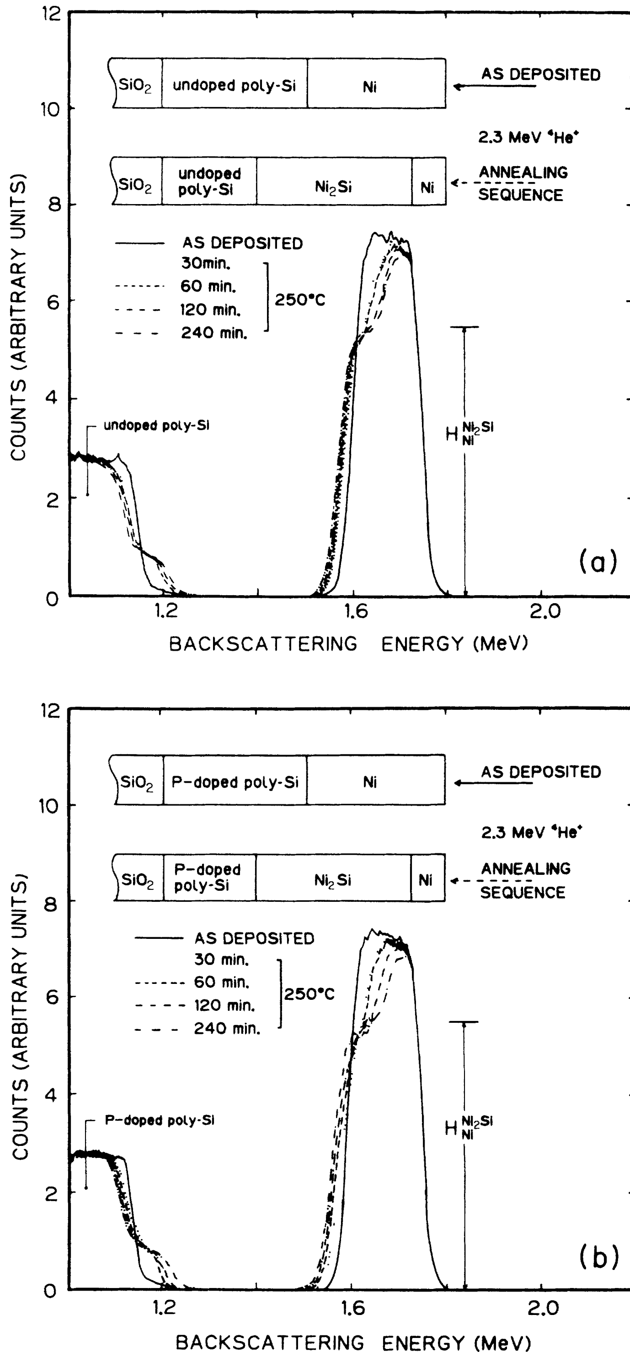

FIG. 1. (a) RBS spectra for Ni_2Si layers grown on undoped polycrystalline Si substrates after different periods of heat treatment at 250 °C, obtained by a 2.3-MeV He^+ ion impinged at a −7° tilt angle and backscattered ions detected at 170°. (b) RBS spectra for Ni_2Si layers on phosphorus-doped polycrystalline Si substrates after heat treatment at 250 °C.

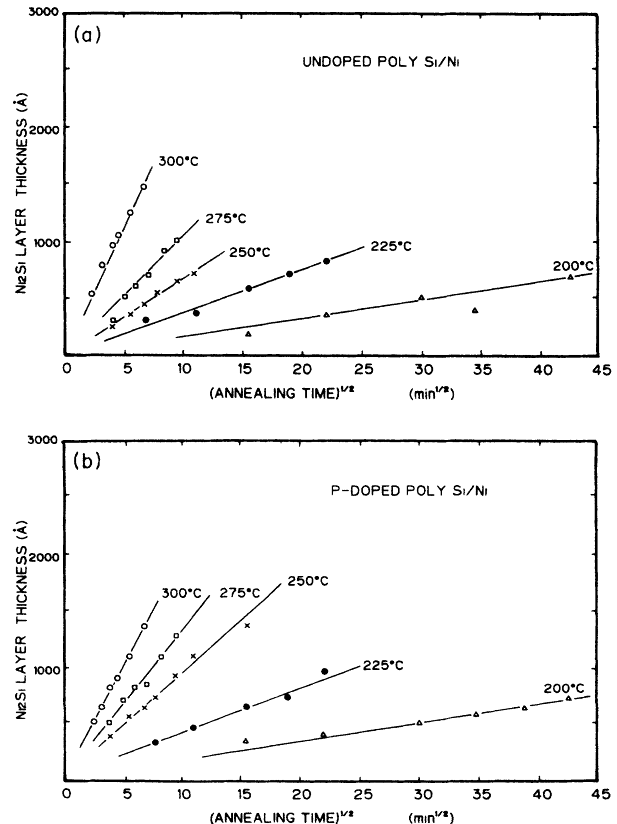

FIG. 2. Ni_2Si layer thickness plotted as a function of the square root of heat treatment time on (a) undoped polycrystalline Si substrates, and (b) phosphorus-doped polycrystalline Si substrates.

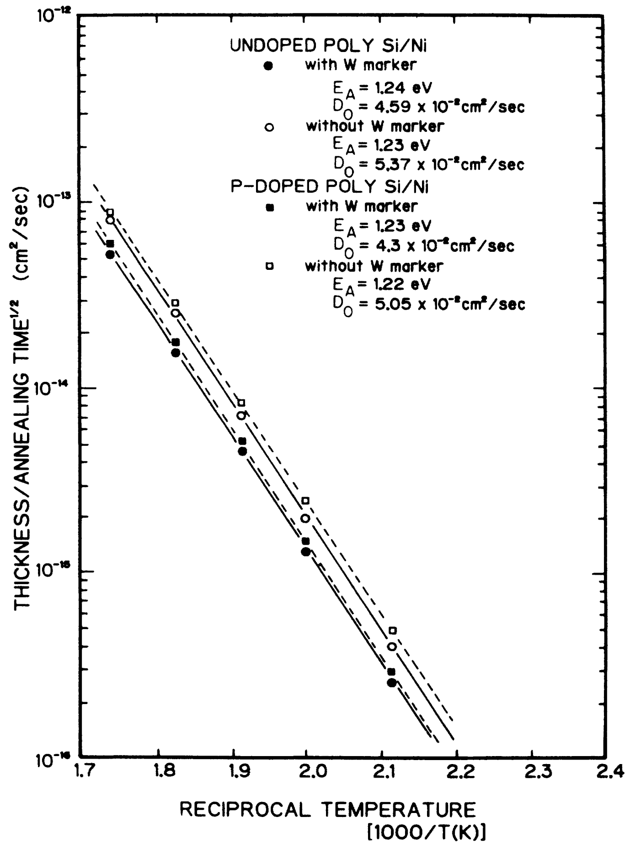

FIG. 3. Arrhenius plots of [(thickness)^2/heat-treatment time] vs reciprocal temperature for Ni_2Si formed on undoped and phosphorus-doped polycrystalline Si substrates. Diffusivities for the samples with a W marker are also plotted.

which can be observed by comparing Fig. 2(a) to Fig. 2(b).

B. Growth kinetics and marker positions of Ni_2Si with the W marker

Rutherford backscattering spectra of Ni_2Si with the W marker on undoped and phosphorus-doped polycrystalline substrates are shown in Figs. 4(a) and 4(b), respectively. According to the height of the plateau in the spectra, it is evident again that the composition of the reacted layers corresponds to that of Ni_2Si.

In Fig. 5, a schematic diagram of a layered growth of Ni_2Si is shown. In the figure, x_1 is the remaining thickness of Ni, x_m is the marker position measured from the surface, and x_2 is the total thickness of Ni and Ni_2Si, so the thickness of Ni_2Si is calculated as $x_\beta = x_2 - x_1$. For marker analysis, we should subtract from x_β the thickness of Ni_2Si formed by the 200 Å of Ni between the W and the Si. Assuming the bulk density for Ni (8.9 g/cm^3), Si (2.33 g/cm^3), and Ni_2Si (7.33 g/cm^3), we can calculate that the reaction of 1 Å of Ni with 0.914 Å of Si forms 1.528 Å of δ-Ni_2Si, so that a compound layer 305.6 Å thick, the layer of $x_2 - x_{2'}$ shown in Fig. 5, is formed by the reaction of 200 Å of Ni with Si.

The kinetics of Ni_2Si on undoped and phosphorus-doped polycrystalline Si substrates is shown in Fig. 6. Here, the compound thickness is calculated from $x_{\beta'}$ ($= x_{2'} - x_1$), where $x_{\beta'}$ means the thickness of silicide which grows beyond the W marker. Also, the heat-treatment time is calculated from $t - t_0$, where t_0 is the time needed for reacting the 200 Å of Ni to form Ni_2Si. The growth kinetics are again governed by a parabolic relation as shown in the figure. The Arrhenius plots for

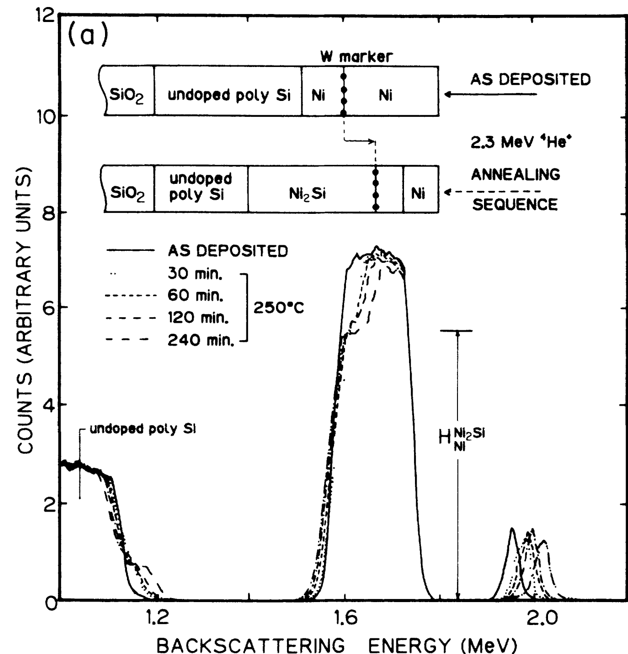

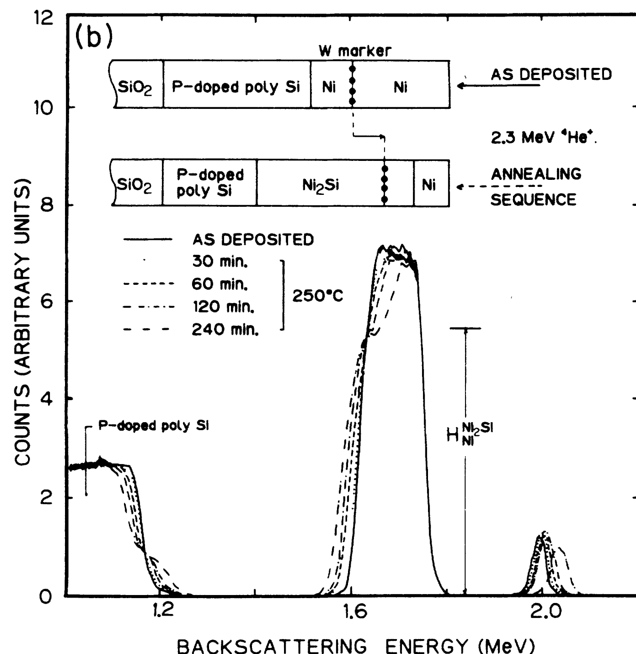

FIG. 4. RBS spectra for Ni_2Si with the W marker grown on (a) undoped and (b) phosphorus-doped polycrystalline Si substrates.

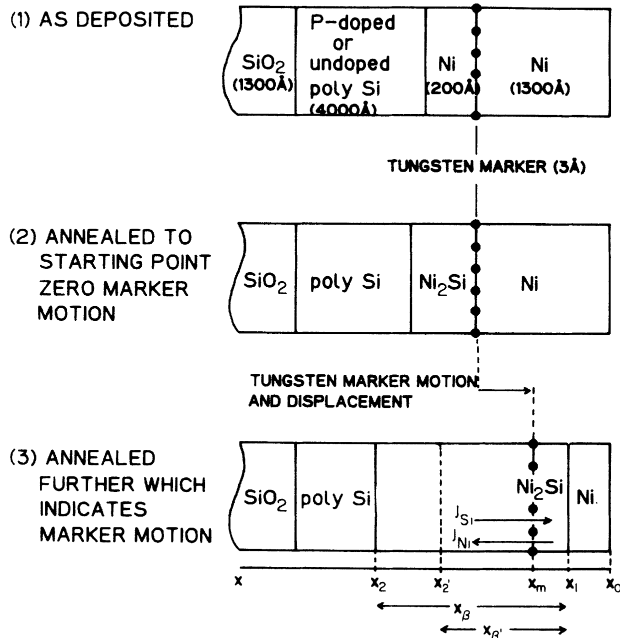

FIG. 5. Schematic diagram of the layered structure containing a marker of nonreacted material (top) and ones after reaction. All distances are referred from the free surface.

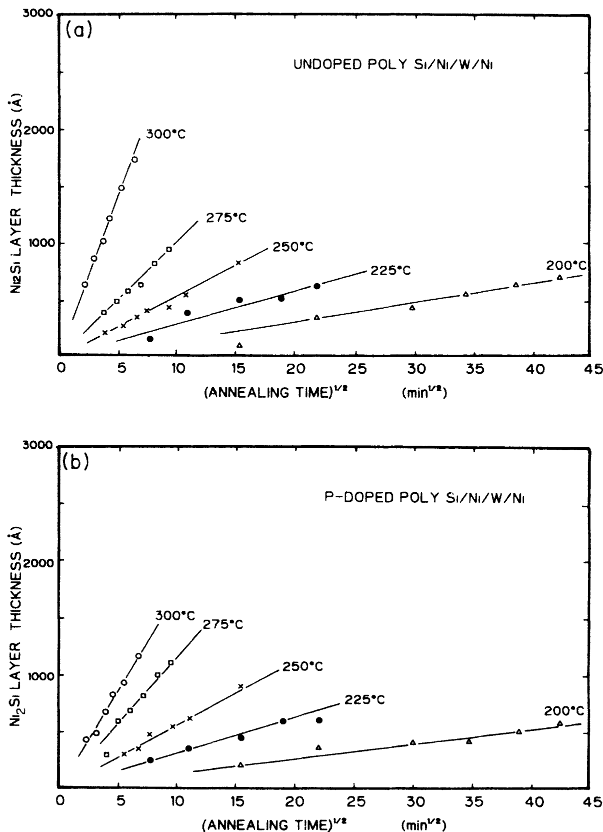

FIG. 6. Time dependence of the thickening of Ni_2Si layers with the W marker on (a) undoped and (b) phosphorus-doped polycrystalline Si substrates.

Ni_2Si with a W marker are also shown in Fig. 3. The activation energies are found to be 1.24 eV for the undoped sample and 1.23 eV for the phosphorus-doped sample. The preexponential factors are 4.59×10^{-2} and 4.3×10^{-2} cm^2/sec, respectively. Again, the growth on the P-doped substrate is faster. We note that the growth of Ni_2Si with the W marker has the same activation energy, but a slightly less preexponential factor, compared to the sample without the marker.

To determine the marker position x_m from a backscattering spectrum,[4] we must first determine the backscattered energy (channel) position C_s of a hypothetical W surface layer by the He^+-ion beam. By combining C_s and the energy-loss parameter of He^+ ions in Ni (i.e., channel/Å of Ni), we can determine the backscattered channel position of C_1 of the W marker below a layer of Ni of thickness x_1. Here, the thickness of unreacted Ni, x_1 in units of Å, is calculated from the following relation:

$$x_1 = x_{\rm Ni} - x_\beta/1.528 , \qquad (1)$$

where $x_{\rm Ni}$ is the initial thickness of deposited Ni and x_β is the total thickness of Ni_2Si. Then the value of x_m can be determined by combining C_1 and the actual backscattered channel position of the W marker, C_m, and the energy-loss parameter of He^+ ions in Ni_2Si (i.e., channel/Å of Ni_2Si) with the procedure as illustrated in Fig. 7.

Briefly, assuming that the energy loss of backscattered He^+ ions per Å of Ni is constant in the energy range and

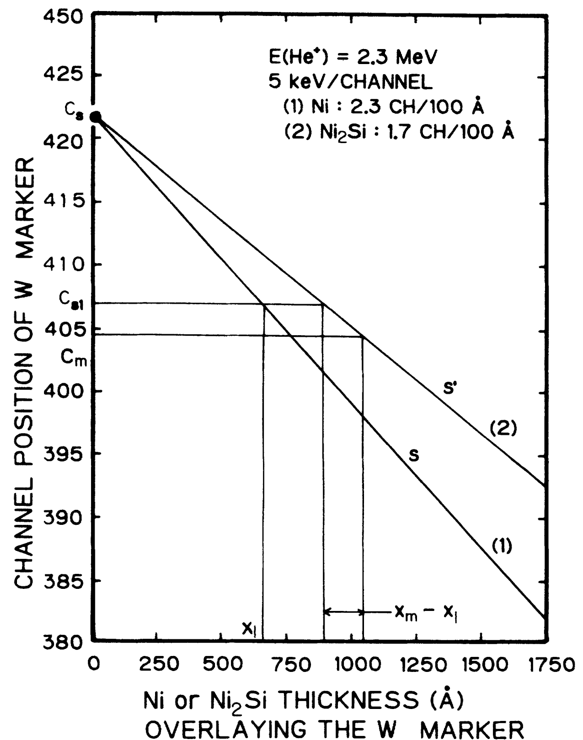

FIG. 7. Graphic method of determining the distance $x_m - x_1$ using the energy-loss parameter of He^+ ions in Ni and Ni_2Si. The energy of incident ions is 2.3 MeV and the conversion factor is 5 keV/channel.

the thickness range used in this experiment, a straight line is drawn using the point C_s and the slope S (channel/Å of Ni). A second straight line is constructed by the point C_s and a slope S' (channel/Å of Ni_2Si), which is again assumed to be constant. Using the value of x_1 calculated from Eq. (1), we obtain the value of C_1 from the line having slope S. The value of C_1 means the incident-ion energy at the Ni/Ni_2Si interface. Finally, we obtain $x_m - x_1$ from the line having the slope S' by knowing C_1 and C_m as illustrated in Fig. 7,

$$x_m = x_1 + (C_s - x_1 S - C_m)/S' . \quad (2)$$

Data of x_m on the undoped and phosphorus-doped polycrystalline Si substrates are plotted as a function of the square root of heat-treatment time in Figs. 8(a) and 8(b), respectively. We find that x_m is linearly dependent on the square root of the time, supporting the fact that the reaction is diffusion controlled.

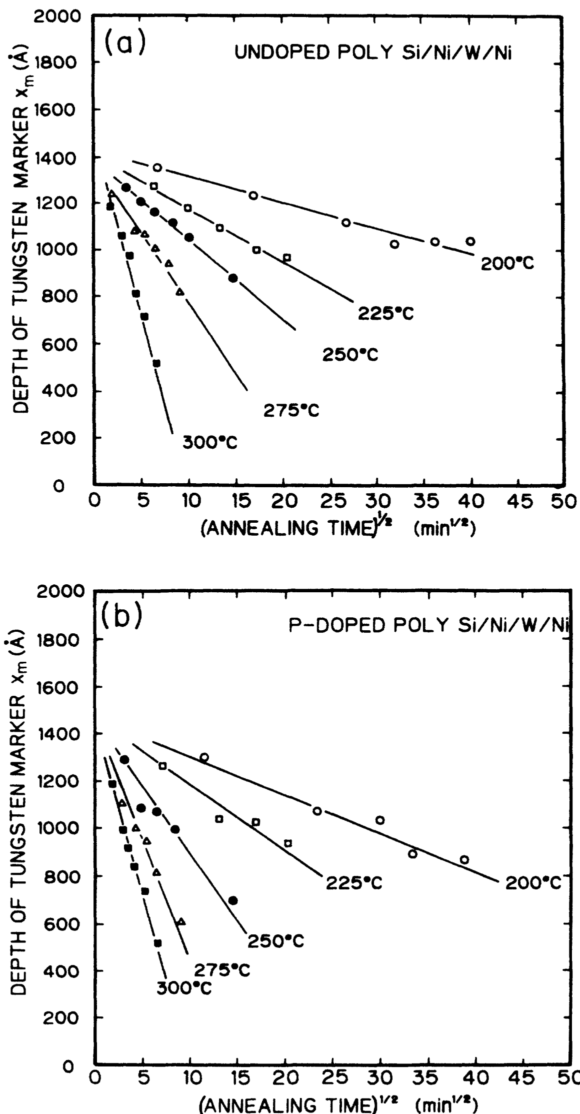

FIG. 8. Time dependence of the W-marker position x_m in Ni_2Si formed on (a) undoped and (b) phosphorus-doped polycrystalline Si substrates.

C. Interfacial drag effect on marker motion

Often, the marker is displaced in the beginning of the reaction by interfacial drag rather than by the difference in diffusional fluxes. The drag effect must be corrected in an accurate analysis.[4] To identify if the marker is dragged and to determine how much the drag is, the data of x_m, x_1, $x_{2'}$, and $x_{\beta'}$ as a function of the fraction of reacted Ni (i.e., x_1/x_{Ni}) are plotted in Fig. 9. In both cases of undoped and phosphorus-doped samples, the line of x_m does not join those of x_1 and $x_{2'}$ at the starting point, where we would expect that $x_1 = x_m = x_{2'}$ if there was no drag. Instead, the line of x_m intercepts the line of $x_{2'}$, and the point of intercept is at a distance of x_d from the line of x_1. We define x_d as the distance of drag, which is about 150 and 275 Å measured from Figs. 9(a) and 9(b), respectively. These values of x_d must be corrected from $x_{2'}$ in the marker analysis. We note that x_d is determined by extrapolation from the line of x_m. This is because the in-depth resolution of RBS is about 200 Å, so the amount and the direction of the early stage of marker displacement cannot be accurately determined. Also, the peak of the marker in RBS has broadened somewhat after the reaction, see Fig. 4.

As shown in Fig. 4, the markers were displaced outward, indicating that Ni is the dominant diffusing species. Also after the subtraction of x_d from $x_m - x_1$, we found that x_m is close to x_1, meaning that the marker is near the Ni_2Si/Ni interface, so the reaction is essentially controlled by the Ni flux. This is in agreement to earlier marker study, where Xe markers were placed in the Si rather than the Ni, and the result had shown Ni to be the dominant diffusing species.

D. Analysis of marker motion

In a diffusion-controlled growth of a layered compound $A_\beta B$ between two elemental phases A and B as depicted in Fig. 5, the two unknowns are the intrinsic interdiffusion coefficients D_A^β and D_B^β, and the two equations which have been derived to solve them are[5]

$$x^2 = 2(1+\beta)\frac{\Delta H_\beta}{kT}\tilde{D}t , \quad (3)$$

and

$$R = \frac{D_A^\beta}{D_B^\beta} = \frac{\beta[(x_2 - x_m) - (x_2^0 - x_m^0)]}{[(x_m - x_1) - (x_m^0 - x_1^0)]} , \quad (4)$$

where x and ΔH_β are, respectively, the thickness and enthalpy of formation of the compound, R is the flux ratio, $\tilde{D}$ is the chemical interdiffusion coefficient given by

$$\tilde{D} = \frac{D_A^\beta}{1+\beta} + \frac{\beta D_B^\beta}{1+\beta} , \quad (5)$$

and x_2^0, x_m^0, and x_1^0 are, respectively, the initial positions of x_2, x_m, and x_1. When there is interfacial drag as shown in Fig. 9 and the initial positions are corrected, we take

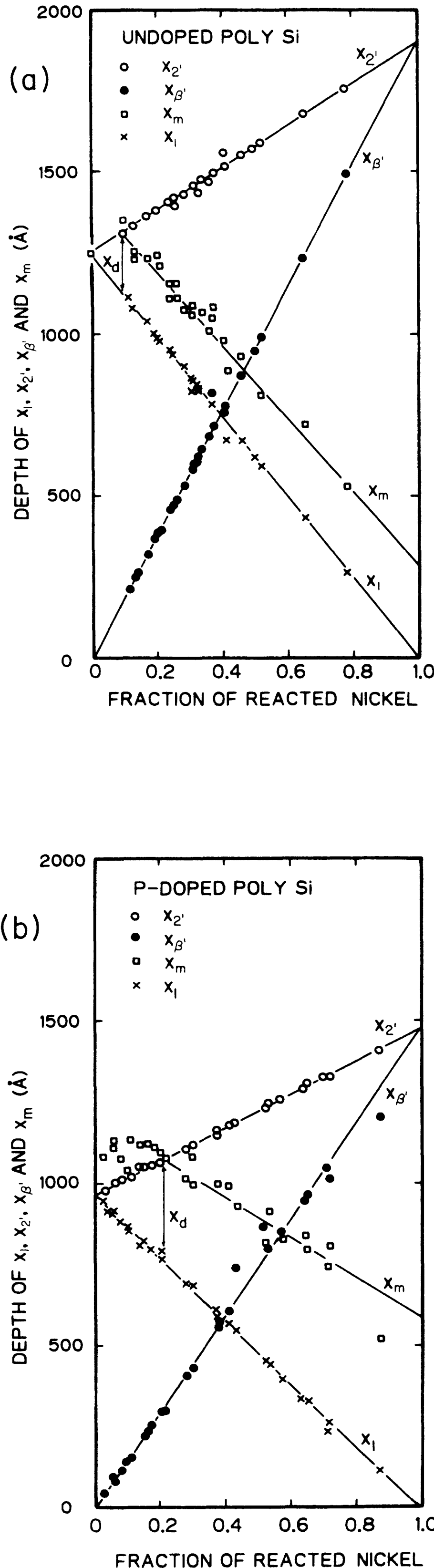

FIG. 9. Plots of fraction of reacted Ni vs x_1, x_m, $x_{2'}$, and $x_{\beta'}$ in order to evaluate the drag effect during the growth of Ni_2Si on (a) undoped and (b) phosphorus-doped polycrystalline Si substrates.

$$R=\frac{D_A^{\beta}}{D_B^{\beta}}=\frac{\beta(x_{2'}-x_m)}{x_m-x_1-x_d}\ . \tag{6}$$

By measuring x and R, we determine D_A^{β} and D_B^{β} from Eqs. (3) and (6). Since x and R have been measured as a function of temperature, the preexponential factor and activation energy of D_A^{β} and D_B^{β} can be obtained from an Arrhenius plot.

In Figs. 10(a) and 10(b), Arrhenius plots of $\tilde{D}$, D_{Si}, and D_{Ni} as a function of the reciprocal temperature for samples on the undoped and phosphorus-doped polycrystalline Si substrates are shown, respectively The activation energies and preexponential factors of the chemical interdiffusion coefficients and intrinsic diffusion coefficients are summarized in Table I.

E. Depth profiles of P, Ni, and Si measured by SIMS

In-depth concentration profiles of P, Ni, and Si in the set of samples (without a W marker) annealed at 250 °C were obtained by SIMS. Figures 11(a) and 11(b) show, respectively, the profiles in as-deposited and after annealing at 250 °C for 4 h. By comparing the profiles, we find that after annealing there is a small concentration gradient of P in the polycrystalline Si, decreasing toward the Ni/Ni_2Si interface, yet there is no pileup of P at any of the interfaces.

The profiles of Ni show a large concentration gradient in the polycrystalline Si decreasing towards the polycrystalline Si/substrate interfaces. It is surprising to find that the gradient exists already in the as-deposited sample. We believe that these gradients were produced by the knock-on effect during the sputter-profiling process since Ni atoms are known to diffuse extremely fast in single-crystal Si.[6] This is evident by a pileup of Ni at the polycrystalline Si/substrate interface in the annealed sample.

IV. DISCUSSION

A. Marker analysis

In general, impurities and solutes can enhance or retard solvent diffusion[7,8] and, in turn, the growth of an intermetallic compound. As shown in Fig. 3, the growth of Ni_2Si on the phosphorus-doped polycrystalline Si substrate is faster than the undoped. We shall first quantify this observation from the data of marker analysis. From Eq. (5) we obtain the following relations:

$$\tilde{D}_{(\text{undoped})}=\frac{D_{Ni}^{UDP}+2D_{Si}^{UDP}}{3}\ , \tag{7}$$

$$\tilde{D}_{(\text{doped})}=\frac{D_{Ni}^{DP}+2D_{Si}^{DP}}{3}\ . \tag{8}$$

Here, D^{UDP} and D^{DP} are defined as intrinsic diffusivities in silicide grown on the undoped and phosphorus-doped polycrystalline Si substrates, respectively. Combining Eqs. (6)–(8), we obtain the ratio of the chemical interdiffusion coefficients between the undoped and phosphorus-doped samples as

$$\frac{\tilde{D}_{(\text{undoped})}}{\tilde{D}_{(\text{doped})}} = \frac{D_{\text{Ni}}^{\text{UDP}} + 2D_{\text{Si}}^{\text{UDP}}}{D_{\text{Ni}}^{\text{DP}} + 2D_{\text{Si}}^{\text{DP}}} = \frac{(R^{\text{UDP}}+2)D_{\text{Si}}^{\text{UDP}}}{(R^{\text{DP}}+2)D_{\text{Si}}^{\text{DP}}} . \quad (9)$$

From Arrhenius plots we obtain

$$D_{\text{Si}}^{\text{UDP}} / D_{\text{Si}}^{\text{DP}} = 0.27$$

and

$$D_{\text{Ni}}^{\text{UDP}} / D_{\text{Ni}}^{\text{DP}} = 1.07 ,$$

for the temperature range investigated in this experiment. Using these values and the R values, we obtain

$$\frac{\tilde{D}_{(\text{undoped})}}{\tilde{D}_{(\text{doped})}} = 0.92 .$$

This calculation thus indicates that the chemical interdiffusion in Ni_2Si on the phosphorus-doped sample is faster by about 8% than that on the undoped sample, and it is due to the influence of P, which increases the diffusion of Si in Ni_2Si by a factor of 3–4. Furthermore, the marker analysis as presented in Table I shows that the major influence from P is on the preexponential factor of Si diffusion and there is no influence on the activation energies. In the next subsection we shall attempt to explain why P affects the preexponential factor of Si diffusion.

In previous studies of Ni_2Si formation,[3,9] the silicide was found to be nonstoichiometric and deficient in Ni.

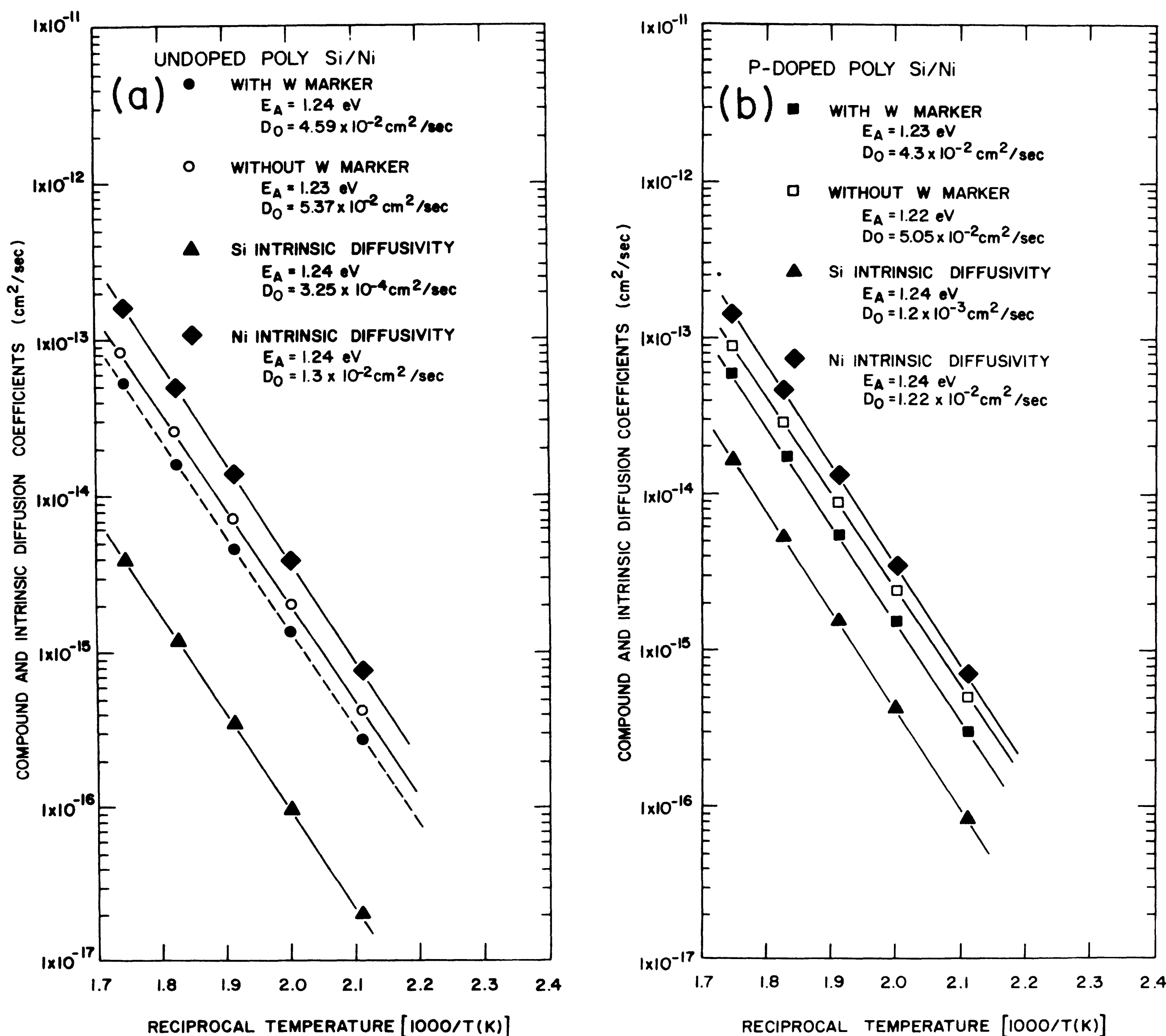

FIG. 10. Intrinsic diffusion coefficients of Ni and Si in Ni_2Si on (a) undoped and (b) phosphorus-doped polycrystalline Si substrates. The chemical interdiffusion coefficients drawn in Fig. 3 are also included as a comparison.

TABLE I. Ni_2Si diffusion coefficients.

Structure	Chemical interdiffusion coefficient D_0 (cm^2/sec)	E_A (eV)	Intrinsic diffusion coefficient D_0 (cm^2/sec)	E_A (eV)
Undoped polycrystalline Si/Ni	5.37×10^{-2}	1.23		
P-doped polycrystalline Si/Ni	5.05×10^{-2}	1.22		
Undoped polycrystalline Si/Ni/W/Ni	4.59×10^{-2}	1.24	Si: 3.25×10^{-4}	1.24
			Ni: 1.3×10^{-2}	1.24
P-doped polycrystalline Si/Ni/W/Ni	4.3×10^{-2}	1.23	Si: 1.2×10^{-3}	1.24
			Ni: 1.22×10^{-2}	1.24

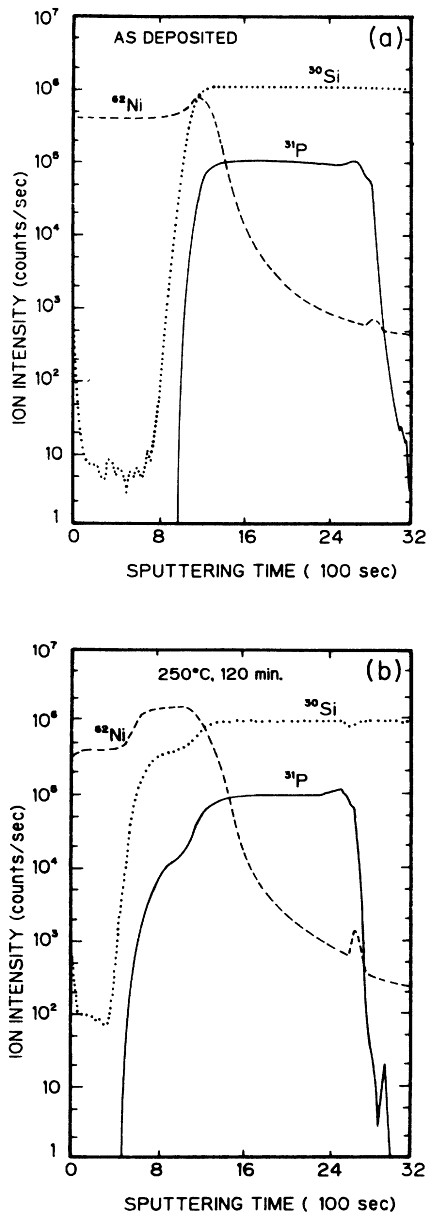

FIG. 11. SIMS profiles of P, Ni, and Si in a Ni_2Si layer formed on a phosphorus-doped polycrystalline Si substrate, (a) as-deposited, and (b) after a heat treatment at 250 °C for 120 min.

The excess vacancies due to the Ni deficiency is responsible for the dominant diffusion of Ni and the less important grain-boundary diffusion in Ni_2Si. In the following analysis, we shall assume a vacancy mechanism of diffusion in the silicide.

B. Correlation effect

We shall first examine the diffusion of Ni and Si in the undoped Ni_2Si. Marker analysis showed that in the undoped case the activation energies for Ni and Si diffusion in Ni_2Si are the same, yet the preexponential factor D_0 for Ni is about 40 times greater than that of Si. Assuming a vacancy mechanism, the general expression of D_0 is[8,10]

$$D_0 = fa^2\nu \exp(S_f + S_m)/k \; , \tag{10}$$

where f is the correlation factor,[11] a is the jump distance, ν is the average jump frequency, S_f and S_m are, respectively, the entropy of formation and migration, and k is Boltzmann's constant. To decide which one of these parameters of D_0 can account for the differences between the Ni and Si diffusion, we shall first examine the crystal structure of Ni_2Si,[12,13] which is a degenerated structure of that of Ni_2In as shown in Fig. 12(a). The diagrams in Figs. 12(b) and 12(c) depict the (001) and (110) planes of Ni_2In, respectively. The crystal structure of Ni_2In can be obtained by stacking its (110) planes according to the sequence as shown in Fig. 12(b). We note that in Ni_2In each In atom has only Ni atoms as the nearest neighbors. The (010) plane of Ni_2Si is shown in Fig. 12(d), which is a deformed (110) plane of Ni_2In. The crystal structure of Ni_2Si is obtained by stacking its (010) plane following the sequence in Fig. 12(b). In Ni_2Si each Si atom has only Ni atoms as the nearest neighbors, but Ni has both Si and Ni; the sublattice of Ni is connected but not the Si sublattice. Therefore, when a Si atom jumps to a neighboring vacant site, it produces a disordered state. Then the next most favorable jump of the Si atom is to return to its original site. In other words, it is a highly correlated jump, which, in general, does not lead to a long-range diffusion. To investigate the correlation effect, we depict in Fig. 13(a) a simplified two-dimensional hexagonal structure where Ni and Si atoms are represented, respectively, by solid and open circles. The ratio of [Ni] to [Si]

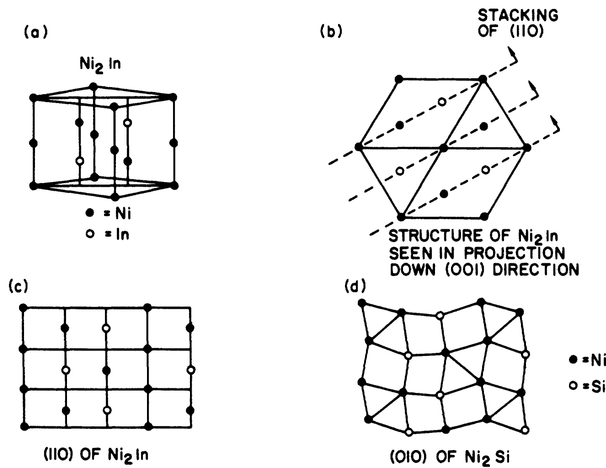

FIG. 12. Crystal structure for (a) a hexagonal unit cell of Ni_2In, (b) Ni_2In seen in a projection down the [001] direction, (c) the (110) plane of Ni_2In, and (d) the (010) plane of Ni_2Si. Panel (b) also shows how the structure of Ni_2In can be generated by a stacking of the (110) planes.

is 2:1. Each Si atom has six Ni atoms, but no Si atoms as the nearest neighbors. Each Ni atom has three Ni and three Si atoms as the nearest neighbors. To introduce a vacancy into the structure, we assume that the vacancy takes a Ni site. This assumption is supported by the fact that during the Ni_2Si growth between a Ni film and Si, there is a deficiency of Ni in the silicide and Ni is the dominant diffusing species. The vacancy is represented by the open square shown in Fig. 13(a).

We consider the exchange of positions between the vacancy and the Ni atoms to the left of the vacancy, and we find that after the exchange each of them keeps the same surroundings as before. Therefore, we denote the exchange frequency between them, which is the same for jumping back and forth, ω_1. This is also true for the other two Ni atoms neighboring the vacancy. On the other hand, if we consider the exchange of positions between the vacancy and the Si atom to the right, the surroundings of each of them changes after the jump and the Si occupies a Ni site. Because such a jump leads to a disordered state, we assume that $\omega_2 \ll \omega_1$, where ω_2 is the frequency of the vacancy jumping from a Ni site to a Si site. After such a jump, the most favorable jump for the vacancy is to return quickly to its original position, and we denote the return frequency ω_4 and we assume that $\omega_4 \gg \omega_1$. Hence, we have $\omega_4 \gg \omega_1 \gg \omega_2$.

To obtain the correlation factors for the Ni and Si atoms diffusing by a vacancy mechanism, we take[14,15]

$$f = \frac{1+\langle \cos\theta_1 \rangle}{1-\langle \cos\theta_1 \rangle} , \tag{11}$$

where $\langle \cos\theta_1 \rangle$ is the mean value of the cosine of the angle between ith and $(i+1)$th jump vectors. For the Ni, the approximate equations are

$$\langle \cos\theta_1 \rangle = \frac{-\omega_1}{3\omega_1+3\omega_2} , \quad f_{\mathrm{Ni}} = \frac{2\omega_1+3\omega_2}{4\omega_1+3\omega_2} \cong \frac{1}{2} . \tag{12}$$

For the Si the approximate equations are

$$\langle \cos\theta_1 \rangle = \frac{-\omega_4}{5\omega_1+\omega_4} , \quad f_{\mathrm{Si}} = \frac{5\omega_1}{5\omega_1+2\omega_4} \cong \frac{5}{2}\frac{\omega_1}{\omega_4} \ll 1 . \tag{13}$$

Since a vacancy occupying a Ni site always has three Ni and three Si atoms as the nearest neighbors (see Fig. 12), the probability P_v of having a vacancy as a nearest neighbor is the same for a Ni or a Si atom. Then, the diffusion

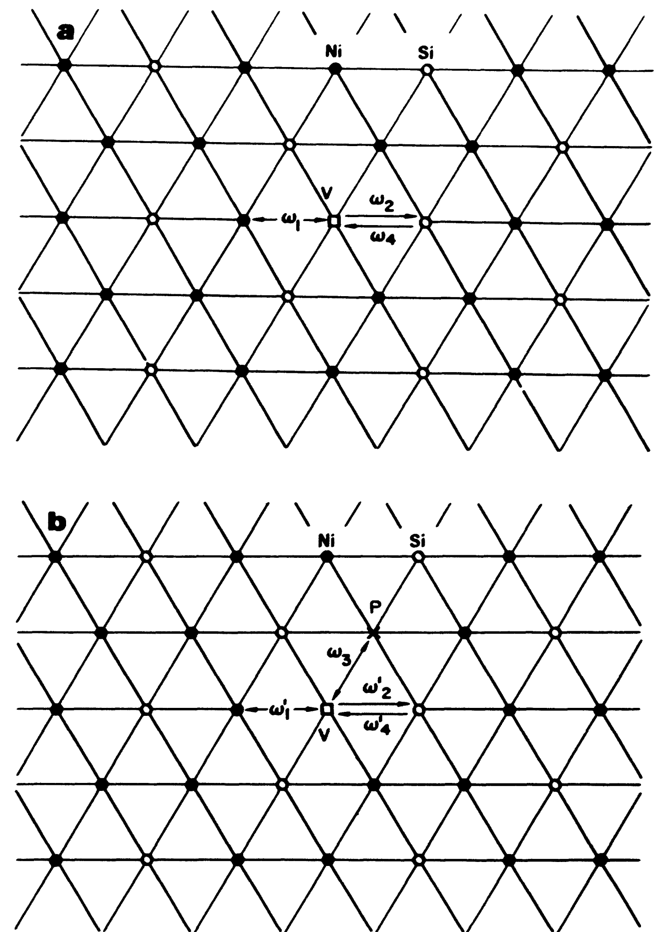

FIG. 13. Schematic diagrams of a two-dimensional hexagonal structure for the consideration of correlation effects in Ni_2Si, where the Ni, Si, and vacancy are represented by solid circles, open circles, and open squares, respectively, and ω_i denotes the exchange frequency as explained in the text. (a) Undoped Ni_2Si, and (b) P-doped Ni_2Si, where a phosphorus atom is represented by the cross.

coefficients for Ni and Si atoms are, respectively,

$$D_{Ni} = f_{Ni} a^2 \omega_1 P_v \ , \quad D_{Si} = f_{Si} a^2 \omega_2 P_v \ . \tag{14}$$

The ratio of D_{Ni}/D_{Si} is obtained by substituting Eqs. (12) and (13) into (14),

$$\frac{D_{Ni}}{D_{Si}} = \frac{1}{5} \frac{\omega_4}{\omega_2} \ . \tag{15}$$

Experimentally, we measured $D_{Ni}/D_{Si} \cong 40$ ($\cong 30$ in a previous measurement);[5] therefore ω_4 is about 2 orders of magnitude greater than ω_2 according to Eq. (15). In turn, it suggests that ω_4, ω_1, and ω_2 are about 1 order of magnitude apart in the relation: $\omega_4 \gg \omega_1 \gg \omega_2$. It is clear that the slow diffusion of Si in Ni_2Si is mainly due to a large ω_4. Hence, a reduction of ω_4 or a reduction of the correlation factor of Si would increase the diffusion of Si.

However, an inspection of Eq. (15) indicates that the ratio of diffusivities, the same as that of jump frequencies, should depend on temperature, yet this is not what has been found in Fig. 10(a). Consequently, while it is tempting to try to argue that the effect of phosphorus is to reduce the correlation factor of Si by using those jumps as shown in Fig. 13(b), the same issue of temperature dependence remains because the data presented in Fig. 10(b) again show no temperature dependence of the ratio of diffusivities. Except, if we make the assumption that the frequency ratios in Ni_2Si are not temperature dependent as in a pure element, we have to use the other factors given in Eq. (10) in order to explain the dopant effect.

We shall now study the dopant effect on the entropy factor of diffusion of Ni and Si. There are two ways of placing a phosphorus atom into the structure, either at a Ni site or a Si site. In the latter case, the P has no Si as the nearest neighbors, so it seems unlikely to have a large effect on the diffusion of Si. For this reason, we will not consider it. Then we are left with the case of both the phosphorus and the vacancy occupying Ni sites as shown in Fig. 13(b). By taking a Ni site, the phosphorus atom always borders three Si atoms. When it joins a vacancy to form a pair, they increase the disorder of the surrounding Si atoms and, in turn, their entropy factor of diffusion. While it is difficult to quantify the effect, it shows qualitatively why P increases the Si diffusion but slightly decreases the Ni diffusion since it occupies a Ni site and reduces some of the excess vacancies. The site occupancy of a substitutional impurity in an intermetallic compound is itself a very important issue and could be studied by using the technique of extended x-ray-absorption fine structure.

On the other hand, since we have measured the preexponential factor, we could use Zener's theory[8] to calculate the entropy factor. Nevertheless, we may not be able to draw a conclusion from it because the silicide has a complicated structure and we are uncertain about the correlation factor.

V. CONCLUSIONS

We conclude the following.

(1) The Ni_2Si growth kinetics on both undoped and phosphorus-doped polycrystalline Si substrates is diffusion controlled. The growth is faster on the phosphorus-doped Si by about 8%.

(2) In the undoped case, analysis of marker motion as a function of time and temperature showed that during the growth of Ni_2Si the intrinsic diffusivity of Ni is greater by a factor of about 40 than that of Si and their difference is in the preexponential factors and not in the activation energies.

(3) In the P-doped case, marker analysis showed that the effect of phosphorus is to increase the preexponential factor of diffusivity of Si by a factor of 4 and to decrease that of Ni very slightly. Again, there is no change in the activation energies.

ACKNOWLEDGMENTS

The authors gratefully acknowledge W. Frey for polycrystalline Si deposition, C. Jahnes for Ni deposition, V. R. Deline for SIMS measurements, P. A. Saudners for RBS measurements, A. A. Levi for various computer programs, P. A. Psaras for technical assistance, and Professor H. Huntington (Rensselaer Polytechnic Institute), S. Pantelides, and D. Gupta for helpful discussions on the correlation factor.

*Present address: Tokyo Denki University, 2-2, Kanda-Nishiki-cho, Chiyoda-ku, Tokyo 101, Japan.

[1] M. Wittmer and K. N. Tu, Phys. Rev. B **29**, 2010 (1984).
[2] P. A. Psaras, R. D. Thompson, S. R. Herd, and K. N. Tu, J. Appl. Phys. **55**, 3536 (1984).
[3] K. N. Tu, W. K. Chu, and J. W. Mayer, Thin Solid Films **25**, 403 (1975).
[4] J. Tardy and K. N. Tu, Phys. Rev. B **32**, 2070 (1985).
[5] U. Gosele, K. N. Tu, and R. D. Thompson, J. Appl. Phys. **53**, 8759 (1982).
[6] R. D. Thompson, D. Gupta, and K. N. Tu, Phys. Rev. B **33**, 2636 (1986).
[7] D. Lazarus, in *Solid State Physics,* edited by F. Seitz and D. Turnbull (Academic, New York, 1960), Vol. 10, p. 71.
[8] P. G. Shewmon, *Diffusion in Solids* (McGraw-Hill, New York, 1963).
[9] J. O. Olowolafe, M.-A. Nicolet, and J. W. Mayer, Thin Solid Films **38**, 143 (1976).
[10] J. R. Manning, *Diffusion Kinetics for Atoms in Crystals* (von Nostrand, Princeton, NJ, 1968).
[11] J. Bardeen and C. Herring, *Atom Movements* (American Society for Metals, Cleveland, 1951), p. 87.
[12] W. B. Pearson, *The Crystal Chemistry and Physics of Metals and Alloys* (Wiley-Interscience, New York, 1972).
[13] R. W. G. Wyckoff, *Crystal Structure* (Interscience, New York, 1963), Vol. 1.
[14] K. Compaan and Y. Haven, Trans. Faraday Soc. **52**, 786 (1956).
[15] H. B. Huntington and P. B. Ghate, Phys. Rev. Lett. **8**, 421 (1962).